JOC The Journal of Organic Chemistry

Article

pubs.acs.org/joc

Molecular Binding Behaviors of Pyromellitic and Naphthalene Diimide Derivatives by Tetrasulfonated 1,5-Dinaphtho-(3*n*+8)-crown-*n* (*n* = 8, 10) in Aqueous Solution

Ling Chen, Ying-Ming Zhang, Li-Hua Wang, and Yu Liu*

Department of Chemistry, State Key Laboratory of Elemento-Organic Chemistry, Nankai University, Tianjin 300071, P.R. China

Supporting Information

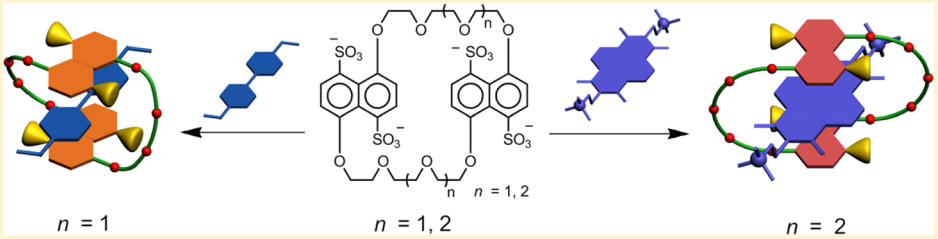

ABSTRACT: The highly affinitive and selective binding processes of tetrasulfonated 1,5-dinaphtho-38-crown-10 ($\mathbf{1}^{4-}$) and tetrasulfonated 1,5-dinaphtho-32-crown-8 ($\mathbf{2}^{4-}$) with pyromellitic diimide and naphthalene diimide derivatives bearing cationic terminal groups ($PMDI^{2+}$ and NDI^{2+}) are comprehensively investigated in aqueous solution by ^1H NMR and UV/vis experiments, mass spectrometry, microcalorimetric titration, and crystallographic analysis. The binding process of host−guest complexation is thermodynamically driven by the large enthalpic gain and favorable entropic change with the high association constants in the range of 10^4−10^6 M^{-1} order of magnitude. Combined with our previously reported thermodynamic data of ethyl viologen (EV^{2+}), it is found that the exclusively selective binding behaviors originate from the size/shape matching effect, as well as the electrostatic interaction between negatively charged hosts and positively charged guests and aromatic π-stacking interrelation between electron-rich donors and electron-deficient acceptors.

INTRODUCTION

The highly ordered and well-defined superstructures organized by multicomponent units have inventive applications in the fabrication of metamaterials and fundamental studies of their unique physio-chemical properties originating from such selective and collective binding process.[1] An impressive progress in this area is to design water-soluble interpenetrated structures using crown ethers, which has been ubiquitously applied to many other macrocyclic cavitands, such as cyclodextrins,[2] cucurbiturils,[3] and cyclophanes.[4] Recently, several research groups have developed a series of water-soluble crown ethers by introducing negatively charged moieties to the macroring of crown ethers.[5] With the aid of supramolecular positive cooperativity, these multiply charged crown ethers can form very stable pseudorotaxane precursors with pyridinium and bipyridinium guests. In particular, we have previously demonstrated that the introduction of sulfonate groups onto the backbone of crown ethers can drastically affect the host−guest binding geometry, endowing these unrigidified macrocyclic compounds with the ability to internally or externally bind toward different cationic substrates.[5e]

A deep insight into the structral freatures and molecular recognition process involving water-soluble crown ethers reveals that these host molecules can be intrinsically considered as negatively charged receptors with electron-rich cavities.[5e] That means some appropiate π-electron deficient molecules bearing positively charged substituents can act as potential guests to selectively bind to tetrasulfonated crown ethers in water. However, up to now, only pyridinium or bipyridinium guests have been employed to synthesize the topologically interpenetrated structures with such water-soluble crown ethers.[5] Among the various aromatic molecules possessing desirable electronic and spectroscopic properties, pyromellitic diimide (PMDI) and naphthalene diimide (NDI) derivatives are widely used as supramolecular building blocks in the construction of thin flims, foldamers, and mechanically interlocked complexes.[6] Motivated by these fascinating resluts, herein we would like to report the supramolecular complexation of tetrasulfonated 1,5-dinaphtho-38-crown-10 ($\mathbf{1}^{4-}$) and tetrasulfonated 1,5-dinaphtho-32-crown-8 ($\mathbf{2}^{4-}$) with two dicationic salts of $PMDI^{2+}$ and NDI^{2+} as a new type of nonpyridinium guests, with the final goal of extending the potential use of water-soluble crown ethers in the construction of functionalized supramolecular assemblies (Chart 1).

RESULTS AND DISCUSSION

UV/vis Spectroscopy and Electrochemical Study. It is well-established that π-stacking interaction between the electron-rich and electron-deficient aromatic components

Received: March 13, 2013
Published: May 2, 2013

   dx.doi.org/10.1021/jo400519z | J. Org. Chem. 2013, 78, 5357−5363

Chart 1. Structures and Proton Designations of Host and Guest Molecules

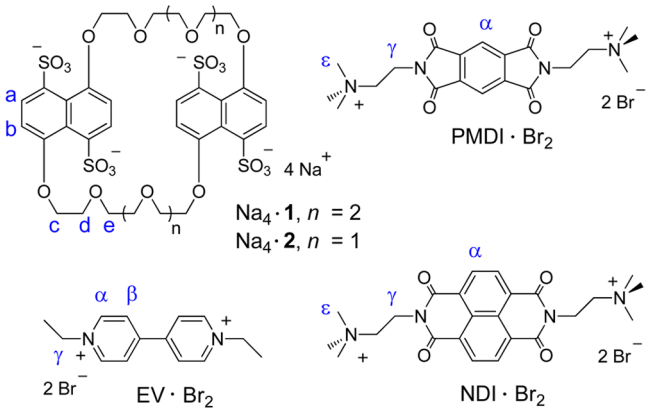

could induce an appreciable charge transfer (CT) absorbance band in the long-wavelength region.[7] As shown in Figure 1a–c,

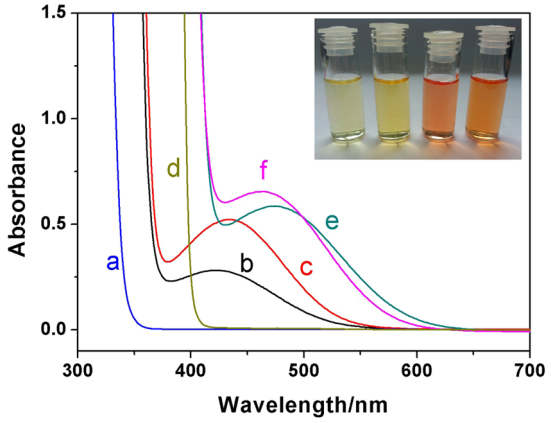

Figure 1. UV/vis absorption spectra of (a) $PMDI^{2+}$, (b) $PMDI^{2+}\subset\mathbf{1}^{4-}$, (c) $PMDI^{2+}\subset\mathbf{2}^{4-}$, (d) NDI^{2+}, (e) $NDI^{2+}\subset\mathbf{1}^{4-}$, and (f) $NDI^{2+}\subset\mathbf{2}^{4-}$ in aqueous solution at 25 °C, respectively ($[\mathbf{1}^{4-}] = [\mathbf{2}^{4-}] = [PMDI^{2+}] = [NDI^{2+}] = 1.0 \times 10^{-3}$ M). (Inset) Visible color changes of $PMDI^{2+}\subset\mathbf{1}^{4-}$, $PMDI^{2+}\subset\mathbf{2}^{4-}$, $NDI^{2+}\subset\mathbf{1}^{4-}$, and $NDI^{2+}\subset\mathbf{2}^{4-}$ (from left to right).

the typical CT absorptions at 422 and 424 nm are clearly observed in the complexes of $PMDI^{2+}\subset\mathbf{1}^{4-}$ and $PMDI^{2+}\subset\mathbf{2}^{4-}$, respectively, indicating the significant $\pi-\pi$ interaction between naphthalenesulfonic moiety as donor and $PMDI^{2+}$ as acceptor. Although these two complexes give a close CT wavelength, the absorption intensity of $PMDI^{2+}\subset\mathbf{2}^{4-}$ ($\varepsilon_{PMDI^{2+}\subset\mathbf{2}^{4-}} = 5.22 \times 10^2$ L·mol^{-1}·cm^{-1}) is much higher than that of $PMDI^{2+}\subset\mathbf{1}^{4-}$ ($\varepsilon_{PMDI^{2+}\subset\mathbf{1}^{4-}} = 2.81 \times 10^2$ L·mol^{-1}·cm^{-1}), implying that there is stronger donor–acceptor interaction in the supramolecular complexation of $\mathbf{2}^{4-}$ with $PMDI^{2+}$. This phenomenon may be attributed to a more rigidified and preorganized cavity of $\mathbf{2}^{4-}$, which facilitates the face-centered stacking arrangements between the tetrasulfonated crown ethers and dicationic $PMDI^{2+}$ in solution. Moreover, it is noteworthy that this CT process could be readily distinguished by not only spectroscopic experiments but also naked eyes. That is, $PMDI^{2+}$ alone is colorless but turns to yellow in the presence of compound $\mathbf{1}^{4-}$ or $\mathbf{2}^{4-}$ (inset photo in Figure 1).

Similarly, the new CT absorption bands centered at 474 nm ($\varepsilon_{NDI^{2+}\subset\mathbf{1}^{4-}} = 5.86 \times 10^2$ L·mol^{-1}·cm^{-1}) and 464 nm ($\varepsilon_{NDI^{2+}\subset\mathbf{2}^{4-}} = 6.54 \times 10^2$ L·mol^{-1}·cm^{-1}) are observed upon addition of equimolar $\mathbf{1}^{4-}$ and $\mathbf{2}^{4-}$ to the aqueous solution of NDI^{2+}, respectively, accompanied by the charareristic color change form colorless to bright red (Figure 1d–f and inset photos). Furthermore, in the case of $NDI^{2+}\subset\mathbf{1}^{4-}$ and $NDI^{2+}\subset\mathbf{2}^{4-}$, both of these complexes display a stronger CT absorption strength and give an obvious bathochromic shift of 52 and 40 nm, respectively, as compared with $PMDI^{2+}\subset\mathbf{1}^{4-}$ and $PMDI^{2+}\subset\mathbf{2}^{4-}$. These observation can be reasonably explained as the larger coplanar π-aromatic conjugate and broader UV absorption of NDI^{2+} in the range from 360 to 420 nm, in which the lower LUMO π-orbital on NDI^{2+} can readily accept the electrons from HOMO π-orbital on the naphthalenesulfonic groups of $\mathbf{1}^{4-}$ and $\mathbf{2}^{4-}$. Moreover, the electrochemical properties of $PMDI^{2+}$ and NDI^{2+} with $\mathbf{1}^{4-}$ and $\mathbf{2}^{4-}$ were investigated by cyclic voltammetry. As shown in Supporting Information Figure S1, the first reduction peaks of $PMDI^{2+}$ and NDI^{2+} show a negative shift in the presence of $\mathbf{1}^{4-}$ and $\mathbf{2}^{4-}$, suggesting the host–guest complexation in aqueous solution.

^{1}H NMR Titration. The binding behaviors of $\mathbf{1}^{4-}$ and $\mathbf{2}^{4-}$ with dicationic guests $PMDI^{2+}$ and NDI^{2+} were further examined by means of ^{1}H NMR titration in D_2O at 25 °C. The chemical shift changes for all the host-guest complexes are summarized in Supporting Information Table S1. As discerned in Figure 2, the proton signals of two complexes ($PMDI^{2+}\subset\mathbf{1}^{4-}$ and $PMDI^{2+}\subset\mathbf{2}^{4-}$) exhibit the fast-exchange equilibrium during ^{1}H NMR time scale. The corresponding chemical shift changes ($\Delta\delta$) take on similar characteristics in all of the protons of $PMDI^{2+}$ upon association with $\mathbf{1}^{4-}$ and $\mathbf{2}^{4-}$; that is, the protons of neighboring methylene linkers (H_γ) underwent a moderate upfield shift upon complexation ($\Delta\delta_{\gamma,PMDI^{2+}\subset\mathbf{1}^{4-}} = -0.23$ ppm and $\Delta\delta_{\gamma,PMDI^{2+}\subset\mathbf{2}^{4-}} = -0.13$ ppm), whereas the ones of aromatic moiety (H_α) gave a pronounced complex-induced upfield shift ($\Delta\delta_{\alpha,PMDI^{2+}\subset\mathbf{1}^{4-}} = -1.07$ ppm and $\Delta\delta_{\alpha,PMDI^{2+}\subset\mathbf{2}^{4-}} = -0.74$ ppm) arising from the mutual diamagnetic shielding effect between aromatic naphthalene and dicationic $PMDI^{2+}$. In this case, the relatively large and flexible cavity of crown ether $\mathbf{1}^{4-}$ could facilitate $PMDI^{2+}$ in stacking with its naphthalene rings at ^{1}H NMR concentration and thus lead to an obvious $\Delta\delta$ value of H_α in complex $PMDI^{2+}\subset\mathbf{1}^{4-}$. There is also a slight downfield shift for the methyl protons (H_ε) of $PMDI^{2+}$ ($\Delta\delta_{\varepsilon,PMDI^{2+}\subset\mathbf{1}^{4-}} = 0.08$ ppm and $\Delta\delta_{\varepsilon,PMDI^{2+}\subset\mathbf{2}^{4-}} = 0.11$ ppm), convincingly

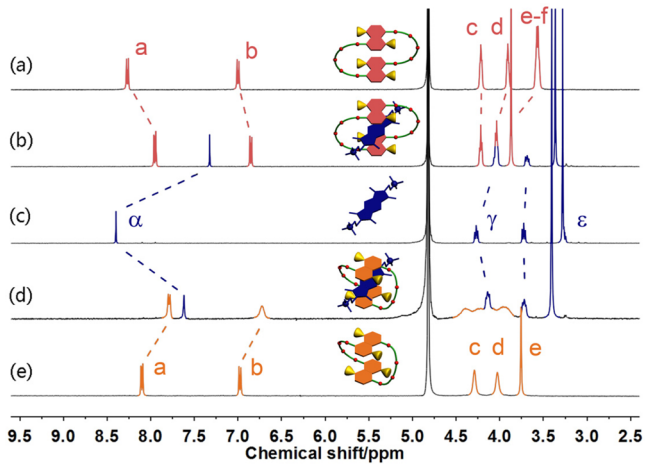

Figure 2. Partial ^{1}H NMR spectra of (a) $\mathbf{1}^{4-}$, (b) $PMDI^{2+}\subset\mathbf{1}^{4-}$, (c) $PMDI^{2+}$, (d) $PMDI^{2+}\subset\mathbf{2}^{4-}$, (e) $\mathbf{2}^{4-}$ in D_2O at 25 °C, respectively (400 MHz, $[\mathbf{1}^{4-}] = [\mathbf{2}^{4-}] = [PMDI^{2+}] = 2.0 \times 10^{-3}$ M).

dx.doi.org/10.1021/jo400519z | J. Org. Chem. 2013, 78, 5357–5363

indicative of the existence of week C−H···O hydrogen bonding interactions between the terminal groups of $PMDI^{2+}$ and oxygen atoms of polyether side chains. Moreover, NMR signals of the crown ether units ($H_{b\text{-}e}$) in complex $PMDI^{2+}\subset\mathbf{2}^{4-}$ are drastically broadened in the range of 3.80−4.49 ppm, which is strikingly distinctive from the ones with a simple pattern of sharp and high-resolution peaks in complex $PMDI^{2+}\subset\mathbf{1}^{4-}$. These phenomena are mainly ascribable to the relatively smaller crown ether cavity of $\mathbf{2}^{4-}$ that thus leads to a slightly rigidified conformation to form close contact with $PMDI^{2+}$ (Figure S2 in the Supporting Information).

The comparative ^{1}H NMR studies of complexes $NDI^{2+}\subset\mathbf{1}^{4-}$ and $NDI^{2+}\subset\mathbf{2}^{4-}$ are shown in Figure 3. Despite the fact that

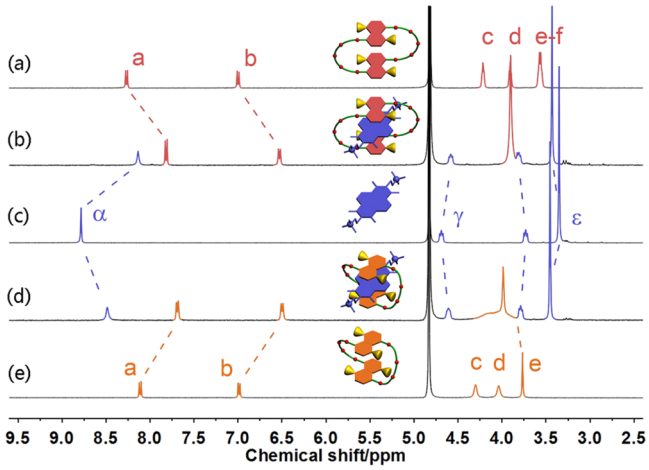

Figure 3. Partial ^{1}H NMR spectra of (a) $\mathbf{1}^{4-}$, (b) $NDI^{2+}\subset\mathbf{1}^{4-}$, (c) NDI^{2+}, (d) $NDI^{2+}\subset\mathbf{2}^{4-}$, (e) **2** in D_2O at 25 °C, respectively (400 MHz, $[\mathbf{1}^{4-}] = [\mathbf{2}^{4-}] = [NDI^{2+}] = 2.0 \times 10^{-3}$ M).

most of proton signals exhibit similar complexation-induced tendency in $NDI^{2+}\subset\mathbf{1}^{4-}$ and $NDI^{2+}\subset\mathbf{2}^{4-}$, there are still some noticeable distinctions. The chemical shifts assigned to the protons of ethylene glycol spacers give significant changes in 1:1 host−guest mixtures of NDI^{2+} with $\mathbf{1}^{4-}$ and $\mathbf{2}^{4-}$. As seen in Figure 3a and b, all the proton signals ($H_{c\text{-}f}$) of tetraethylene glycol chains in $\mathbf{1}^{4-}$ are integrated to a single resonance peak at 3.90 ppm, whereas the ones of triethylene glycol linkers in $\mathbf{2}^{4-}$ are located as a broad peak in the range from 3.81 to 4.34 ppm. Moreover, as compared with the $\Delta\delta$ values of aromatic protons in $PMDI^{2+}\subset\mathbf{1}^{4-}$ and $PMDI^{2+}\subset\mathbf{2}^{4-}$, the corresponding values of H_a and H_b are larger in the case of $NDI^{2+}\subset\mathbf{1}^{4-}$ ($\Delta\delta_{a,NDI^{2+}\subset\mathbf{1}^{4-}} = -0.45$ ppm and $\Delta\delta_{b,NDI^{2+}\subset\mathbf{1}^{4-}} = -0.47$ ppm) and $NDI^{2+}\subset\mathbf{2}^{4-}$ ($\Delta\delta_{a,NDI^{2+}\subset\mathbf{2}^{4-}} = -0.42$ ppm and $\Delta\delta_{b,NDI^{2+}\subset\mathbf{2}^{4-}} = -0.49$ ppm), implying that the large-sized guest of NDI^{2+} makes a significant impact in spatially controlling the intrerrelation between the electron-rich and electron-deficient moieties (Figure S2 in the Supporting Information). On the other hand, the aromatic protons H_γ in complex $NDI^{2+}\subset\mathbf{1}^{4-}$ give a upfield shift with a remarkable $\Delta\delta$ value ($\Delta\delta_{\gamma,NDI^{2+}\subset\mathbf{1}^{4-}} = -0.65$ ppm), which is two times larger than the corresponding value in complex $NDI^{2+}\subset\mathbf{2}^{4-}$ ($\Delta\delta_{\gamma,NDI^{2+}\subset\mathbf{2}^{4-}} = -0.29$ ppm). In contrast to crown ether $\mathbf{2}^{4-}$ with a smaller cavity, there is enough space in the larger cavity of $\mathbf{1}^{4-}$ to effectively accommodate the aromatic core of NDI^{2+}, ultimately resulting in the relatively stronger shielding effect and sizable upfield shifts originating from the cooperative π-stacking interaction in the complex of $NDI^{2+}\subset\mathbf{1}^{4-}$.

Crystal Structures. By the slow vapor diffusion of acetone into aqueous solution of the corresponding ion−ion electrostatic salts, two crystalline complexes of $PMDI^{2+}\subset\mathbf{1}^{4-}$ and $NDI^{2+}\subset\mathbf{1}^{4-}$ were obtained to further investigate their binding behaviors in the solid state.[8] The crystallographic complex of $PMDI^{2+}\subset\mathbf{1}^{4-}$ is comprised of one host and two guest molecules as its chemical formula, where one $PMDI^{2+}$ is naturally located in the crystal lattice, and the other $PMDI^{2+}$ is axially interpenetrated into the crown ether rings and stabilized by a combination of $\pi-\pi$ stacking and C−H···O hydrogen-bonding interactions. As shown in Figure 4a, the naphthalene ring in

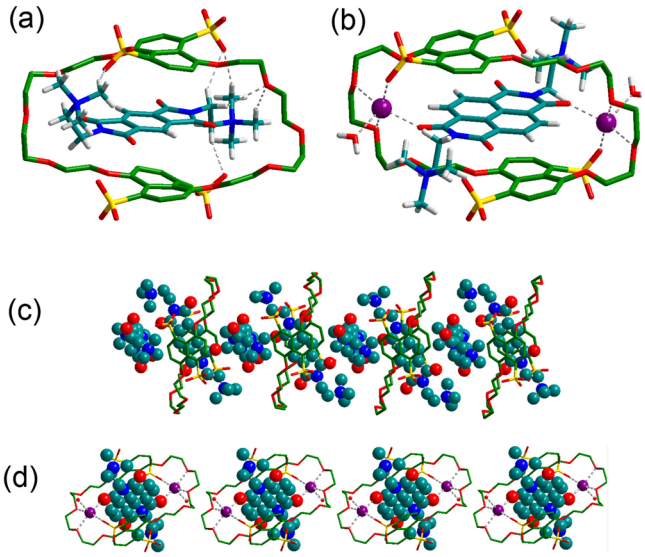

Figure 4. Crystal structures of [2]pseudorotaxane (a) $PMDI^{2+}\subset\mathbf{1}^{4-}$ and (b) $NDI^{2+}\subset\mathbf{1}^{4-}$, and packing representation of (c) $PMDI^{2+}\subset\mathbf{1}^{4-}$ and (d) $NDI^{2+}\subset\mathbf{1}^{4-}$. Solvent molecules and partial hydrogen atoms are omitted for clarity.

crystal $PMDI^{2+}\subset\mathbf{1}^{4-}$ adopts two possible conformations involving the π-donor−acceptor interaction with the phenyl center and diimide fragment of $PDMI^{2+}$. It is generally accepted that a closer distance of donor−acceptor stacking arrangements is more favorable for the effective aromatic $\pi-\pi$ interactions in the superstructure of $PMDI^{2+}\subset\mathbf{1}^{4-}$. In our case, the average planes of two naphthalene rings are approximately parallel to the external face of $PMDI^{2+}$ with the interplanar spacings of 3.45 and 3.47 Å,[9] respectively, which are very close to the reported separation between naphthalene and $PMDI^{2+}$ pairs in the range from 3.35 to 3.42 Å.[10] Meanwhile, there are extensive intermolecular C−H···O hydrogen-bonding networks[11] between the ammonium terminal group of $PMDI^{2+}$ and oxygen atoms of polyether chains in $\mathbf{1}^{4-}$ to jointly fix the relative orientation in the [2]pseudorotaxane of $PMDI^{2+}\subset\mathbf{1}^{4-}$.

On the contrary, the single crystal structure of $NDI^{2+}\subset\mathbf{1}^{4-}$ is obtained as a different chemical formula of $NDI^{2+}\cdot Na_2\cdot\mathbf{1}^{4-}$ (Figure 4b). Two sodium ions are located out of the crown ether ring as counterions, and each of them is stabilized by two oxygen atoms of glycol side chain of $\mathbf{1}^{4-}$, one sulfonate, one water molecule, and one oxygen atom of NDI^{2+} (Figure S2−S5 in the Supporting Information). Although the existence of sodium ion as competetive guest may decrease the close contact of positively charged ammonium salts with negatively charged sulfonates in the crystal lattices, the favorable π-stacking interaction still takes place between NDI^{2+} plane and disulfonated naphthalene with a perfect face-centroid distance

dx.doi.org/10.1021/jo400519z | J. Org. Chem. 2013, 78, 5357−5363

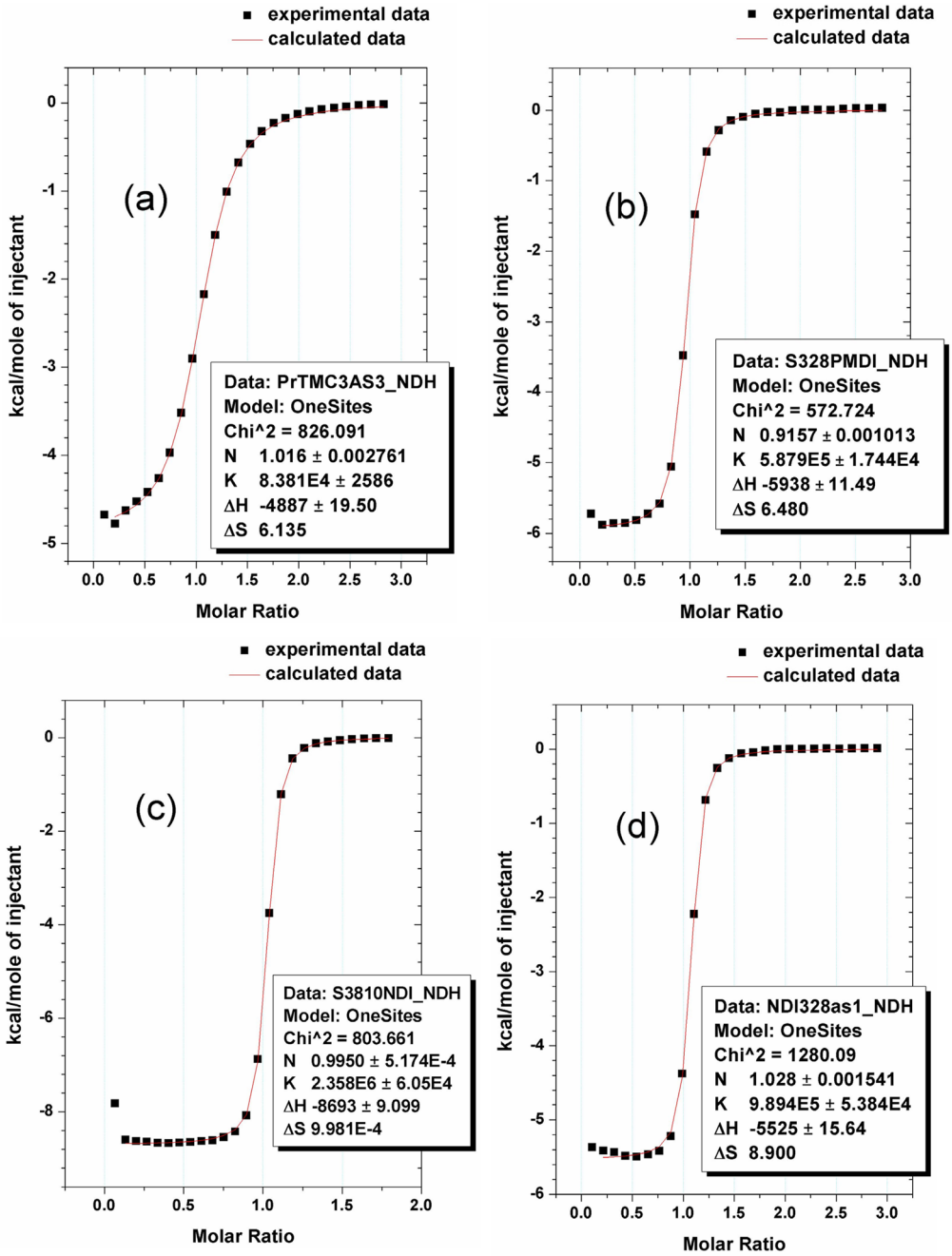

Figure 5. ITC experiments on complexation of (a) $PMDI^{2+}\subset \mathbf{1}^{4-}$, (b) $PMDI^{2+}\subset \mathbf{2}^{4-}$, (c) $NDI^{2+}\subset \mathbf{1}^{4-}$, and (d) $NDI^{2+}\subset \mathbf{2}^{4-}$, respectively, in neat water at 25 °C.

Table 1. Associate Constants (K_a/M^{-1}), Standard Free Energy ($\Delta G°$/kJ·mol^{-1}), Enthalpy ($\Delta H°$/kJ·mol^{-1}) and Entropy Changes ($T\Delta S°$/kJ·mol^{-1}) for 1:1 Inclusion Complexation in Water at 25 °C

complexes	K_a	$-\Delta G°$	$-\Delta H°$	$T\Delta S°$
$EV^{2+}\subset \mathbf{1}^{4-a}$	(1.85 ± 0.04) × 10^5	30.06 ± 0.05	27.20 ± 0.01	2.86 ± 0.07
$PMDI^{2+}\subset \mathbf{1}^{4-b}$	(8.08 ± 0.30) × 10^4	27.99 ± 0.09	20.59 ± 0.15	7.40 ± 0.24
$NDI^{2+}\subset \mathbf{1}^{4-b}$	(2.33 ± 0.03) × 10^6	36.32 ± 0.03	36.31 ± 0.04	0.01 ± 0.01
$EV^{2+}\subset \mathbf{2}^{4-a}$	(5.25 ± 0.58) × 10^7	40.04 ± 0.28	41.54 ± 0.54	2.50 ± 0.26
$PMDI^{2+}\subset \mathbf{2}^{4-b}$	(5.82 ± 0.05) × 10^5	32.90 ± 0.02	24.85 ± 0.01	8.05 ± 0.03
$NDI^{2+}\subset \mathbf{2}^{4-b}$	(9.81 ± 0.08) × 10^5	34.18 ± 0.02	23.17 ± 0.03	11.01 ± 0.08

[a]Reference 5e. [b]This work.

of 3.40 Å.[12] Moreover, it should be noted that, apart form the predominant aromatic π-stacking interaction, there is no obvious hydrogen-bonding interconnection in this [2]-pseudorotaxane structure of $NDI^{2+}\subset \mathbf{1}^{4-}$, mainly due to the

dx.doi.org/10.1021/jo400519z | J. Org. Chem. 2013, 78, 5357−5363

competitive contribution of sodium ions to constrain the spatial orientation between ammonium units of NDI^{2+} and oxygen atoms of $\mathbf{1}^{4-}$. Furthermore, it is noteworthy that the existence of sodium ion is not an indispensable part for the complexation of NDI^{2+} with $\mathbf{1}^{4-}$ in solution, because the binding strength of $\mathbf{1}^{4-}$ with NDI^{2+} decreases to a certain extent in the presence of excess sodium bromide (Figure S6 in the Supporting Information).

Association Constants and Thermodynamics. The molecular binding process and thermodynamic origins of tetrasulfonated crown ether $\mathbf{1}^{4-}$ and $\mathbf{2}^{4-}$ with two dicationic guests of $PMDI^{2+}$ and NDI^{2+} were quantitatively investigated by the method of isothermal titration calorimetry (ITC) measurements in aqueous solution (Figure 5). For a comparative purpose, those thermodynamic parameters for $\mathbf{1}^{4-}$ and $\mathbf{2}^{4-}$ with bipyridinium salt of ethyl viologen (EV^{2+}) in our previous work are also listed in Table 1. As discerned from Table 1, the equilibrium association constants (K_a) of crown ether $\mathbf{1}^{4-}$ with three guests are in the range from 10^4 to 10^6 M^{-1} order of magnitude, whereas those for crown ether $\mathbf{2}^{4-}$ can reach up to 10^7 M^{-1}, showing a good host–guest selectivity in the molecular recognition process. Concretely, the K_a values for complexation with all the guests decrease in the following order.

$$\mathbf{1}^{4-}\text{: } NDI^{2+} > EV^{2+} > PMDI^{2+}$$

$$\mathbf{2}^{4-}\text{: } EV^{2+} > NDI^{2+} > PMDI^{2+}$$

Combined with the aforementioned spectroscopic analysis, it is not surprising that the two crown ethers $\mathbf{1}^{4-}$ and $\mathbf{2}^{4-}$ can display different selective abilities toward the dicationic substrates in water. Since the two crown ethers are essentially considered as negative charged receptors with electron-rich cavity, the structure-dependent binding process mainly depends on the aromatic π-stacking and electrostatic attraction. In our previous work, we have demonstrated that the intramolecular charge repulsion is a decisive factor to preorganize the structures of water-soluble crown ethers.[5e] Compared to $PMDI^{2+}$ and NDI^{2+} possessing a flexible alkyl chain, two pyridinium units in EV^{2+} are a cyclic π-conjugation system to increase its rigidity and delocalize the intensive positive charges on the whole bipyridinium plane. This structural feature makes EV^{2+} more electrons deficient to significantly reduce the intramolecular charge repulsion upon binding with host $\mathbf{2}^{4-}$. In addition, benefiting from a better host–guest size-fit efficiency, the suitable NDI^{2+} aromatic core could adequately occupy the crown ether cavity of $\mathbf{1}^{4-}$ to achieve the intense aromatic π-stacking interaction, ultimately resulting in the highest affinity among all the examined dicationic guests.

Thermodynamically, the binding process of host–guest association is governed in a favorable way with negative enthalpy ($-\Delta H^\circ$ = 20.59–41.54 kJ mol^{-1}) and positive entropy change ($T\Delta S^\circ$ = 0.01–11.01 kJ mol^{-1}), as shown in Table 1. Although the complexation of $\mathbf{2}^{4-}$ with EV^{2+} and $PMDI^{2+}$ gives more favorable enthalpy gains ($\Delta H^\circ_{EV^{2+}\subset\mathbf{1}^{4-}} - \Delta H^\circ_{EV^{2+}\subset\mathbf{2}^{4-}}$ = 14.34 kJ mol^{-1} and $\Delta H^\circ_{PMDI^{2+}\subset\mathbf{1}^{4-}} - \Delta H^\circ_{PMDI^{2+}\subset\mathbf{2}^{4-}}$ = 4.26 kJ mol^{-1}), this situation is distinctly different in the case of $\mathbf{1}^{4-}$ and $\mathbf{2}^{4-}$ with NDI^{2+} ($\Delta H^\circ_{NDI^{2+}\subset\mathbf{1}^{4-}} - \Delta H^\circ_{NDI^{2+}\subset\mathbf{2}^{4-}} = -13.14$ kJ mol^{-1}). The dominant enthalpy changes imply that the π-stacking interaction working at the aromatic rings and hydrogen-bonding interconnection are two decisive factors to govern the molecular recognition process in aqueous solution. In our case, considering that all the hosts and guests in our present study have the same charge numbers and similar molecular structures, the size/shape matching upon supramolecular complexation must be responsible for the large disparities of enthalpy changes in complex $NDI^{2+}\subset\mathbf{1}^{4-}$. That means, the large-sized of $\mathbf{1}^{4-}$ prefers to trap NDI^{2+} by a joint contribution of noncovalent interactions, leading to a closer and compacter aromatic π-stacking between donor and acceptor. Accordingly, the existence of face-to-face π-stacking interaction in the interpenetrated structure of $NDI^{2+}\subset\mathbf{1}^{4-}$ is well confirmed in both aqueous solution and the solid state, as previously identified by the spectroscopic analyses and crystallographic structures.

Along with the enthalpy changes, the complexation of $\mathbf{1}^{4-}$ and $\mathbf{2}^{4-}$ with EV^{2+}, $PMDI^{2+}$, and NDI^{2+} is also entropically favored ($T\Delta S^\circ > 0$) in the range from 0.01 to 11.01 kJ mol^{-1}. The electrostatic attraction between tetrasulfonated crown ethers and dicationic substrates, as well as the conformational freedom change upon host–guest complexation, leads to the entropy-controlled binding process. It can be found that there is a comparative entropy gain in the complexation of $\mathbf{1}^{4-}$ and $\mathbf{2}^{4-}$ with EV^{2+} and $PMDI^{2+}$ ($T\Delta S^\circ_{EV^{2+}\subset\mathbf{1}^{4-}} - T\Delta S^\circ_{EV^{2+}\subset\mathbf{2}^{4-}} = 0.36$ kJ mol^{-1} and $T\Delta S^\circ_{PMDI^{2+}\subset\mathbf{1}^{4-}} - T\Delta S^\circ_{PMDI^{2+}\subset\mathbf{2}^{4-}} = -0.65$ kJ mol^{-1}). Therefore, benefiting from the large enthalpy change, the standard free energies (ΔG°) in $EV^{2+}\subset\mathbf{2}^{4-}$ and $PMDI^{2+}\subset\mathbf{2}^{4-}$ are remarkably higher than the ones in $EV^{2+}\subset\mathbf{1}^{4-}$ and $PMDI^{2+}\subset\mathbf{1}^{4-}$ ($\Delta G^\circ_{EV^{2+}\subset\mathbf{1}^{4-}} - \Delta G^\circ_{EV^{2+}\subset\mathbf{2}^{4-}}$ = 9.98 kJ mol^{-1} and $\Delta G^\circ_{PMDI^{2+}\subset\mathbf{1}^{4-}} - \Delta G^\circ_{PMDI^{2+}\subset\mathbf{2}^{4-}}$ = 4.91 kJ mol^{-1}). In contrast, the entropy gain is strikingly different in the complexation of NDI^{2+} with $\mathbf{1}^{4-}$ and $\mathbf{2}^{4-}$ ($T\Delta S^\circ_{NDI^{2+}\subset\mathbf{1}^{4-}} - T\Delta S^\circ_{NDI^{2+}\subset\mathbf{2}^{4-}} = -11.00$ kJ mol^{-1}), which overwhelms the apparently favorable enthalpy change in $NDI^{2+}\subset\mathbf{1}^{4-}$ and thus leads to nearly the same ΔG° value as $NDI^{2+}\subset\mathbf{2}^{4-}$ ($\Delta G^\circ_{NDI^{2+}\subset\mathbf{1}^{4-}} - \Delta G^\circ_{NDI^{2+}\subset\mathbf{2}^{4-}} = -2.14$ kJ mol^{-1}). These phenomena could be ascribable to size/shape matching arising from the host–guest complementarity. The orderly threading of NDI^{2+} makes the accommodated guest molecules more immovable in the crown ether cavity, and consequently, this conformational fixation results in the large entropic loss upon complexation with host $\mathbf{1}^{4-}$. Comparatively, the incorporation of rigidified and small-sized host $\mathbf{2}^{4-}$ with the larger coplanar π-aromatic core of NDI^{2+} could be forced into a distorted conformation, which may induce extensive disorder in solution to achieve a closer electrostatic contact between quaternary ammonium cations and sulfonated sites and thus give favorable entropic gain for complex $NDI^{2+}\subset\mathbf{2}^{4-}$.

Selective Binding Behaviors. The significant differences in association constants and thermodynamic origins of the water-soluble crown ethers toward dicationic guests enable us to further construct multicomponent assemblies in water. Two groups of model complexes with high affinity and ring-size selectivity, $NDI^{2+}\subset\mathbf{1}^{4-}$ ($K_S^{NDI^{2+}\subset\mathbf{1}^{4-}} = 2.33 \times 10^6$ M^{-1}) and $EV^{2+}\subset\mathbf{2}^{4-}$ ($K_S^{EV^{2+}\subset\mathbf{2}^{4-}} = 5.25 \times 10^7$ M^{-1}), were chosen to investigate the specific binding behaviors in the supramolecular architectures.[13] The equimolar mixture of hosts ($\mathbf{1}^{4-}$ and $\mathbf{2}^{4-}$) and guests (EV^{2+} and NDI^{2+}) was preliminarily explored by ^1H NMR titration method to determine the dominant supramolecular species in solution. As judged from Figure 6c, the resonances of aromatic protons of NDI^{2+} ($H_{\alpha,NDI^{2+}}$) and EV^{2+} ($H_{\alpha,EV^{2+}}$ and $H_{\beta,EV^{2+}}$) in the equimolar mixture are observed at 8.14, 8.62, and 7.77 ppm, respectively, which resembles the simple superposition of $NDI^{2+}\subset\mathbf{1}^{4-}$ and $EV^{2+}\subset\mathbf{2}^{4-}$ in Figure 6b and d. However, the corresponding signals at 8.48, 8.62, and

dx.doi.org/10.1021/jo400519z | J. Org. Chem. 2013, 78, 5357–5363

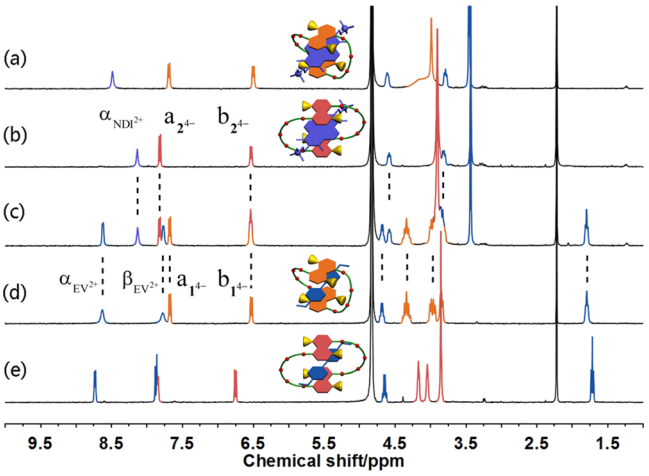

Figure 6. Partial ^{1}H NMR spectra of (a) NDI^{2+} and $\mathbf{2}^{4-}$, (b) NDI^{2+} and $\mathbf{1}^{4-}$, (c) NDI^{2+}, EV^{2+}, $\mathbf{1}^{4-}$, and $\mathbf{2}^{4-}$, (d) EV^{2+} and $\mathbf{2}^{4-}$, and (e) EV^{2+} and $\mathbf{1}^{4-}$ in D_2O at 25 °C, respectively (400 MHz, $[\mathbf{1}^{4-}] = [\mathbf{2}^{4-}] = [NDI^{2+}] = [EV^{2+}] = 2.0 \times 10^{-3}$ M).

7.77 ppm for $NDI^{2+}\subset\mathbf{2}^{4-}$ and $EV^{2+}\subset\mathbf{1}^{4-}$ could not be observed in the quaternary system (Figure 6a and e). Combined with those distinguishable resonances of nonaromatic protons, it is rationalized that the size-dependent complexes $NDI^{2+}\subset\mathbf{1}^{4-}$ and $EV^{2+}\subset\mathbf{2}^{4-}$ can spontaneously reach a selective binding process in water, while the proportion of $NDI^{2+}\subset\mathbf{2}^{4-}$ and $EV^{2+}\subset\mathbf{1}^{4-}$ is very small and therefore cannot be accurately identified.

On the other hand, ESI-MS experiments were carried out to examine this selective binding process. As expected, the peaks at m/z 539.0905, 695.1551, and 1391.3189 could be clearly assigned to $[(NDI^{2+} + \mathbf{1}^{4-})/2]^-$, $[(EV^{2+} + \mathbf{2}^{4-})/2]^-$, and $[NDI^{2+} + \mathbf{1}^{4-} + H^+]^-$, respectively (Figure S11–S13 in the Supporting Information). Moreover, only moderate MS peak for $[(EV^{2+} + \mathbf{1}^{4-})/2]^-$ is observed at m/z 583.1156, and no peak assigned to $NDI^{2+}\subset\mathbf{2}^{4-}$ could be found, despite the fact that $NDI^{2+}\subset\mathbf{2}^{4-}$ shows somewhat higher K_a value than $EV^{2+}\subset\mathbf{1}^{4-}$ (Figure S14 and S15 in the Supporting Information). These results jointly indicate that the complexation of $\mathbf{1}^{4-}$ with NDI^{2+} and $\mathbf{2}^{4-}$ with EV^{2+} is the predominant process in solution. Moreover, on the basis of the thermodynamic parameters in Table 1, the reliable thermodynamic properties for this selective binding process can be calculated as $K_a = 6.63 \times 10^2$ M^{-1}, $\Delta H° = -27.43$ kJ·mol^{-1}, and $T\Delta S° = -11.28$ kJ·mol^{-1} (see the Supporting Information), convincingly demonstrating that this binding process is strongly enthalpy driven, accompanied by the unfavorable entropy change. This can be supported by the fact that the noncovalent driving forces and extensive loss of conformational freedom upon host–guest binding together contribute to the pronounced enthalpic gain and entropic loss in this selective binding process.

CONCLUSION

In conclusion, the selective molecular binding behaviors between the water-soluble crown ethers ($\mathbf{1}^{4-}$ and $\mathbf{2}^{4-}$) and two dicationic substrates as a new type of nonpyridinium guests ($PMDI^{2+}$ and NDI^{2+}) are systematically evaluated, giving a thermodynamically favorable complexation with K_a values in the order of magnitude from 10^4 to 10^6 M^{-1}. The binding affinity of $PMDI^{2+}$, NDI^{2+}, and EV^{2+} with $\mathbf{1}^{4-}$ and $\mathbf{2}^{4-}$ shows that the effective utilization of size/shape matching in conjunction with other noncovalent interaction, such as electrostatic attraction and aromatic π-stacking interaction, is one of crucial and basic factors to govern the specific molecular recognition process, which could be further allowed to construct a quaternary system with selective binding behaviors. These obtained results in this work are very useful in our effort to consistently understand the structure–activity relationship of water-soluble crown ethers and will expedite the development of crown ether-based molecular devices in aqueous media.

EXPERIMENTAL SECTION

General Method. All chemicals were commercially available unless noted otherwise. Host compounds $\mathbf{1}^{4-}$ and $\mathbf{2}^{4-}$ were used with sodium salts, and guest molecules EV^{2+}, $PMDI^{2+}$, and NDI^{2+} were used with bromine salts. NMR data were recorded on 400 MHz spectrometer. All chemical shifts were referenced to the internal acetone signal at 2.22 ppm.[14] Absorption spectra were recorded on a UV/vis spectrometer. The cyclic voltammetry measurements were carried out at 25 °C on an electrochemical analyzer in 0.1 M NaCl aqueous solution as supporting electrolyte. The working electrode was glassy carbon, the counter electrode was Pt coil, and the reference electrode was Ag/AgCl electrode, respectively. The sample concentration was 1.0×10^{-3} M and the scan rate was set to 100 mV/s. Mass spectra were performed on Q-TOF LC/MS (ESI). All of the X-ray intensity data were collected on a rotating anode diffractometer equipped with a CCD Area Detector System, using monochromated Mo-Ka (λ = 0.71073 Å) radiation at T = 113(2) K. CCDC No. 875326 and 916257 contain the supplementary crystallographic data of this work. These data can be obtained free of charge from the Cambridge Crystallographic Data Centre via www.ccdc.cam.ac.uk/data_request/cif.

A thermostatted and fully computer-operated isothermal calorimetry (VP-ITC) instrument was used for all the microcalorimetric experiments. The ITC experiments were performed at 25 °C in aqueous solution, giving the association constants (K_a) and the thermodynamic parameters of guests upon complexation. In each run, a solution of guest in a 0.250 mL syringe was sequentially injected with stirring at 300 rpm into a solution of host in the sample cell (1.4227 mL volume). A control experiment to determine the heat of dilution was carried out for each run by performing the same number of injections with the same concentration of guest compound as used in the titration experiments into a same solution without the host compound. The dilution enthalpies determined in control experiments were subtracted from the enthalpies measured in the titration experiments to obtain the net reaction heat. All thermodynamic parameters reported in this work were obtained by using the "one set of binding sites" model. Two independent titration experiments were performed to afford self-consistent parameters and to give the averaged values.

Synthesis of $PMDI^{2+}$ and NDI^{2+} Bromine Salts. *N*,*N*-Dimethylethylenediamine (2.42 g, 27.4 mmol) in 30 mL of DMF was added dropwise during 10 min to a solution of pyromellitic dianhydride (3.00 g, 13.7 mmol) in 50 mL DMF. The reaction mixture was heated to refluxing for a 4 h. After cooled, iodomethane (10 mL) was added and maintained at 60 °C for further 12 h. The precipitate was afforded and filtered, and then washed with dichloromethane (100 mL) and diethyl ether (100 mL). The iodine salt of $PMDI^{2+}$ was afforded as yellow solid. Then, the counterion iodine was changed to bromine according to the reported literatures[15] in yield 67%. The dicationic guest of NDI^{2+} bromine salt was synthesized by a similar procedure in yield 46%. The characterization data of $PMDI^{2+}$ and NDI^{2+} bromine salts were in accordance with the reported ones.[16]

ASSOCIATED CONTENT

Supporting Information

Cyclic voltammetric curves, X-ray crystallographic data of $PMDI^{2+}\subset\mathbf{1}^{4-}$ and $NDI^{2+}\subset\mathbf{1}^{4-}$ in CIF format, molecular sizes in crystal structures, calorimetric titration curves, as well as ESI-MS spectra of the quaternary system. This material is available free of charge via the Internet at http://pubs.acs.org.

dx.doi.org/10.1021/jo400519z | J. Org. Chem. 2013, 78, 5357–5363

AUTHOR INFORMATION

Corresponding Author

*E-mail: yuliu@nankai.edu.cn.

Notes

The authors declare no competing financial interest.

ACKNOWLEDGMENTS

This work was finacially supported by 973 Program (2011CB932500), NNSFC (No. 20932004 and 91227107).

REFERENCES

(1) (a) Badjić, J. D.; Balzani, V.; Credi, A.; Silvi, S.; Stoddart, J. F. *Science* **2004**, *303*, 1845−1849. (b) Zhu, X.-Z.; Chen, C.-F. *J. Am. Chem. Soc.* **2005**, *127*, 13158−13159. (c) Loeb, S. J. *Chem. Soc. Rev.* **2007**, *36*, 226−235. (d) Dsouza, R. N.; Pischel, U.; Nau, W. M. *Chem. Rev.* **2011**, *111*, 7941−7980. (e) Safont-Sempere, M. M.; Fernández, G.; Würthner, F. *Chem. Rev.* **2011**, *111*, 5784−5814. (f) Zheng, B.; Wang, F.; Dong, S.; Huang, F. *Chem. Soc. Rev.* **2012**, *41*, 1621−1636. (g) Yan, X.; Wang, F.; Zheng, B.; Huang, F. *Chem. Soc. Rev.* **2012**, *41*, 6042−6065. (h) Yang, W.; Li, Y.; Liu, H.; Chi, L.; Li, Y. *Small* **2012**, *8*, 504−516.

(2) (a) Wenz, G.; Han, B. H.; Müller, A. *Chem. Rev.* **2006**, *106*, 782−817. (b) Harada, A.; Hashidzume, A.; Yamaguchi, H.; Takashima, Y. *Chem. Rev.* **2009**, *109*, 5974−6023. (c) Chen, Y.; Liu, Y. *Chem. Soc. Rev.* **2010**, *39*, 495−505.

(3) (a) Lagona, J.; Mukhopadhyay, P.; Chakrabarti, S.; Isaacs, L. *Angew. Chem., Int. Ed.* **2005**, *44*, 4844−4870. (b) Rekharsky, M. V.; Yamamura, H.; Kawai, M.; Osaka, I.; Arakawa, R.; Sato, A.; Ko, Y. H.; Selvapalam, N.; Kim, K.; Inoue, Y. *Org. Lett.* **2006**, *8*, 815−818. (c) Liu, Y.; Shi, J.; Chen, Y.; Ke, C.-F. *Angew. Chem., Int. Ed.* **2008**, *47*, 7293−7296. (d) Zhang, Z.-Z.; Zhang, Y.-M.; Liu, Y. *J. Org. Chem.* **2011**, *76*, 4682−4685.

(4) (a) Au-Yeung, H. Y.; Pantoş, G. D.; Sanders, J. K. M. *Proc. Natl. Acad. Sci. U.S.A.* **2009**, *106*, 10466−10470. (b) Fang, L.; Basu, S.; Sue, C.-H.; Fahrenbach, A. C.; Stoddart, J. F. *J. Am. Chem. Soc.* **2011**, *133*, 396−399. (c) Li, H.; Fahrenbach, A. C.; Coskun, A.; Zhu, Z.; Barin, G.; Zhao, Y.; Botros, Y. Y.; Sauvage, J.-P.; Stoddart, J. F. *Angew. Chem., Int. Ed.* **2011**, *50*, 6782−6788. (d) Yu, G.; Xue, M.; Zhang, Z.; Li, J.; Han, C.; Huang, F. *J. Am. Chem. Soc.* **2012**, *134*, 13248−13251. (e) Yu, G.; Zhou, X.; Zhang, Z.; Han, C.; Mao, Z.; Gao, C.; Huang, F. *J. Am. Chem. Soc.* **2012**, *134*, 19489−19497.

(5) (a) Hoffart, D. J.; Tiburcio, J.; de la Torre, A.; Knight, L. K.; Loeb, S. J. *Angew. Chem., Int. Ed.* **2008**, *47*, 97−101. (b) Lestini, E.; Nikitin, K.; Müller-Bunz, H.; Fitzmaurice, D. *Chem.—Eur. J.* **2008**, *14*, 1095−1106. (c) Ji, X.; Li, J.; Chen, J.; Chi, X.; Zhu, K.; Yan, X.; Zhang, M.; Huang, F. *Macromolecules* **2012**, *45*, 6457−6463. (d) Chen, L.; Zhang, Y.-M; Liu, Y. *J. Phys. Chem. B* **2012**, *116*, 9500−9506. (e) Chen, L.; Zhang, H.-Y.; Liu, Y. *J. Org. Chem.* **2012**, *77*, 9766−9773. (f) Ji, X.; Zhang, M.; Yan, X.; Li, J.; Huang, F. *Chem. Commun.* **2013**, 1178−1180.

(6) (a) Vignon, S. A.; Jarrosson, T.; Iijima, T.; Tseng, H.-R.; Sanders, J. K. M.; Stoddart, J. F. *J. Am. Chem. Soc.* **2004**, *126*, 9884−9885. (b) Han, T.; Chen, C.-F. *J. Org. Chem.* **2007**, *72*, 7287−7293. (c) Bhosale, S. V.; Jani, C. H.; Langford, S. J. *Chem. Soc. Rev.* **2008**, *37*, 331−342. (d) Mullen, K. M.; Davis, J. D.; Beer, P. D. *New J. Chem.* **2009**, *33*, 769−776. (e) Jacquot de Rouville, H.-P.; Iehl, J.; Bruns, C. J.; McGrier, P. L.; Frasconi, M.; Sarjeant, A. A.; Stoddart, J. F. *Org. Lett.* **2012**, *14*, 5188−5191.

(7) (a) Hunter, C. A.; Lawson, K. R.; Perkins, J.; Urch, C. J. *J. Chem. Soc., Perkin Trans. 2* **2001**, 651−669. (b) Martinez, C. R.; Iverson, B. L. *Chem. Sci.* **2012**, *3*, 2191−2201.

(8) Crystal data for $PMDI^{2+}\subset\mathbf{1}^{4-}$: $C_{76}H_{114}N_8O_{38.25}S_4$ M = 1879.99, triclinic, space group *P*2(1)/*c*, *a* = 18.452(5), *b* = 21.012(5), *c* = 23.169(5) Å, α = 77.835(13)°, β = 76.289(13)°, γ = 80.419(14)°, *V* = 8467(4) Å^3, *F*(000) = 3984, *Z* = 4, D_c = 1.475 g cm^{-3}, μ = 0. 211 mm^{-1}, approximate crystal dimensions, 0.26 × 0.20 × 0.08 mm3, θ range = 1.82−25.02°, 78323 measured reflections, of which 29686 (R_{int} = 0.0877) were unique, final *R* indices [$I > 2\sigma(I)$]: R_1 = 0.0932, wR_2 = 0.2373, *R* indices (all data): R_1 = 0.1366, wR_2 = 0.2709, goodness of fit on F^2 = 1.088. Crystal data for $NDI^{2+}\subset\mathbf{1}^{4-}$: $C_{30}H_{38}N_2NaO_{14.50}S_2$ M = 745.73, monoclinic, space group *P*2(1)/*c*, *a* = 16.0646(16), *b* = 19.1312(18), *c* = 14.7690(12) Å, α = 90°, β = 114.212(4)°, γ = 90°, *V* = 4139.8(7) Å^3, *F*(000) = 1564, *Z* = 4, D_c = 1.197 g cm^{-3}, μ = 0.199 mm^{-1}, approximate crystal dimensions, 0.20 × 0.18 × 0.16 mm^3, θ range = 1.75−27.88°, 42648 measured reflections, of which 9853 (R_{int} = 0.0474) were unique, final *R* indices [$I > 2\sigma(I)$]: R_1 = 0.1088, wR_2 = 0.3177, *R* indices (all data): R_1 = 0.1231, wR_2 = 0.3289, goodness of fit on F^2 = 1.070.

(9) This average distance is measured between the center of symmetry of distorted sulfonated 1,5-dinaphthol on $\mathbf{1}^{4-}$ and $PMDI^{2+}$ plane. The closest distances ($d_{C6-PMDI}$ = 3.25 Å and $d_{C20-PMDI}$ = 3.31 Å) between 1,5-dinaphthol and $PMDI^{2+}$ are shorter than the average value.

(10) (a) Hamilton, D. G.; Feeder, N.; Prodi, L.; Teat, S. J.; Clegg, W.; Sanders, J. K. M. *J. Am. Chem. Soc.* **1998**, *120*, 1096−1097. (b) Hansen, J. G.; Feeder, N.; Hamilton, D. G.; Gunter, M. J.; Becher, J.; Sanders, J. K. M. *Org. Lett.* **2000**, *2*, 449−452. (c) Liu, Y.; Klivansky, L. M.; Khan, S. I.; Zhang, X. *Org. Lett.* **2007**, *9*, 2577−2580.

(11) The C−H···O hydrogen-bonding parameters are shown as follows: H···O distance (Å), C−H···O angle (deg), C···O distance (Å): 2.50, 165.5, 3.45; 2.47, 145.8, 3.34; 2.53, 153.7, 3.43; 2.32, 163.2, 3.28; 2.58, 161.0, 3.52; and 2.75, 155.3, 3.67.

(12) This average distance is measured between the center of symmetry of distorted sulfonated 1,5-dinaphthol on $\mathbf{1}^{4-}$ and NDI^{2+} plane. The closest distance (d_{C6-NDI} = 3.36 Å) between 1,5-dinaphthol and $PMDI^{2+}$ is shorter than the average value.

(13) (a) Wu, A.; Isaacs, L. *J. Am. Chem. Soc.* **2003**, *125*, 4831−4835. (b) Hwang, I.-W.; Kamada, T.; Ahn, T. K.; Ko, D. M.; Nakamura, T.; Tsuda, A.; Osuka, A.; Kim, D. *J. Am. Chem. Soc.* **2004**, *126*, 16187−16198. (c) Jiang, W.; Winkler, H. D. F.; Schalley, C. A. *J. Am. Chem. Soc.* **2008**, *130*, 13852−13853. (d) Wang, F.; Han, C.; He, C.; Zhou, Q.; Zhang, J.; Wang, C.; Li, N.; Huang, F. *J. Am. Chem. Soc.* **2008**, *130*, 11254−11255. (e) Chas, M.; Gil-Ramírez, G.; Ballester, P. *Org. Lett.* **2011**, *13*, 3402−3405. (f) Zeng, J.; Wang, W.; Deng, P.; Feng, W.; Zhou, J.; Yang, Y.; Yuan, L.; Yamato, K.; Gong, B. *Org. Lett.* **2011**, *13*, 3798−3801. (g) Li, C.; Shu, X.; Li, J.; Fan, J.; Chen, Z.; Weng, L.; Jia, X. *Org. Lett.* **2012**, *14*, 4126−4129. (h) Ji, X.; Yao, Y.; Li, J.; Yan, X.; Huang, F. *J. Am. Chem. Soc.* **2013**, *135*, 74−77.

(14) Gottlieb, H. E.; Kotlyar, V.; Nudelman, A. *J. Org. Chem.* **1997**, *62*, 7512−7515.

(15) Neelakandan, P. P.; Hariharan, M.; Ramaiah, D. *Org. Lett.* **2005**, *7*, 5765−5768.

(16) (a) Au-Yeung, H. Y.; Pantoş, G. D.; Sanders, J. K. M. *Angew. Chem., Int. Ed.* **2010**, *49*, 5331−5334. (b) Au-Yeung, H. Y.; Pengo, P.; Pantoş, G. D.; Otto, S.; Sanders, J. K. M. *Chem. Commun.* **2009**, 419−421.